ARTICIES

https://doi.org/10.1038/s41929-022-00784-5



OPEN

Facile access to fused 2D/3D rings via intermolecular cascade dearomative [2 + 2] cycloaddition/rearrangement reactions of quinolines with alkenes

Jiajia Ma¹,⁴, Shuming Chen [©]2,³,⁴, Peter Bellotti [©]1,⁴, Tobias Wagener¹, Constantin Daniliuc¹, Kendall N. Houk [©]2 and Frank Glorius [©]1 [™]

Hybrid fused two-dimensional/three-dimensional (2D/3D) rings are important pharmacophores in drugs owing to their unique structural and physicochemical properties. Preparation of these strained ring systems often requires elaborate synthetic effort and exhibits low efficiency, thus representing a limiting factor in drug discovery. Here, we report two types of energy-transfer-mediated cascade dearomative [2+2] cycloaddition/rearrangement reactions of quinoline derivatives with alkenes, which provide a straightforward avenue to 2D/3D pyridine-fused 6-5-4-3- and 6-4-6-membered ring systems. Notably, this energy-transfer-mediated strategy features excellent diastereoselectivity that bypasses the general reactivity and selectivity issues of photochemical [2+2] cycloaddition of various other aromatics. Tuning the aza-arene substitutions enabled selective diversion of the iridium photocatalysed energy transfer manifold towards either cyclopropanation or cyclobutane-rearrangement products. Density functional theory calculations revealed a cascade energy transfer scenario to be operative.

ing systems are key pharmacophores in drugs and bioactive natural products and have found high prevalence among more than 95% of marketed drugs^{1,2}. Two-dimensional (2D) aromatic rings such as benzene and pyridine rank among the most commonly occurring scaffolds^{3,4}. The three-dimensional (3D) aliphatic 3-, 4-, 5- and 6-membered rings follow behind but have recently attracted increasing attention in drug discovery (Fig. 1a) due to their modest molecular weight, improved solubility and physicochemical profile^{5,6}. Furthermore, this poorly populated chemical space offers unmatched opportunities in skeletal diversification at the core of diversity-oriented synthesis7. In this context, fused ring systems with hybrid 2D and 3D fragments, possessing unique structural and physicochemical properties, have emerged as important scaffolds in medicinal chemistry (Fig. 1b). For example, varenicline, based on a hybrid 2D/3D fused 6-6-5-6 ring, has been marketed to treat smoking addiction and MK-8886, based on a hybrid 2D/3D fused 6-5-3 ring, has been invented by Merck for the treatment of type 2 diabetes mellitus and has recently entered clinical trials8. Additionally, many other compounds containing fused 2D/3D rings are currently under pre-clinical validation or clinical trials⁹⁻¹⁴. However, the preparation of such polycyclic molecules—especially those featuring high ring strain-often exhibits low efficiency and often requires elaborate synthetic efforts, which is a rate-limiting factor in drug discovery and development^{15,16}. To this end, the advancement of general and straightforward synthetic methods towards fused 2D/3D rings featuring readily available feedstock resources, good generality and high reaction efficiency/selectivity is of great interest.

The de novo synthesis of ring systems is often based on cycloaddition reactions. The exergonic cycloadditions of 1,3-dienes with alkenes, capable of generating various ring systems, are amongst the most fundamental transformations in synthetic chemistry^{17,18}. Recently, this classical realm has witnessed rapid advancements owing to the introduction of aromatics as reactants by the visible-light energy-transfer process¹⁹⁻³³. Stemming from our reported [4+2]-dearomative cycloaddition between aza-arenes and alkenes²⁹, we questioned whether the established reactivity could be diverted towards a cascade dearomative cycloaddition/rearrangement reaction forming unusual fused 2D/3D rings (Fig. 1c). In this context, quinolines are recognized as suitable reactants due to the potentially divergent ortho/para/meta cycloaddition reactivity and the innate presence of pharmaceutically relevant N-heterocycles. More specifically, the carbocyclic ring of quinolines is initially proposed to couple with alkenes in a [2+2] fashion under energy-transfer conditions. This endergonic process will lead to an enthalpy increased and more reactive vinylpyridine intermediate, which could easily undergo further cycloadditions or rearrangements by a consecutive energy transfer, thus leading to diverse sp³-carbon-rich ring systems³⁴. This proposed cascade dearomative cycloaddition/rearrangement (CDACR) reaction offers an ideal approach towards pyridine-fused 2D/3D rings. It is worth noting that, despite the fact that the intramolecular photochemical [2+2]cycloaddition of a benzenoid ring has been disclosed35-37 and its great potential was demonstrated in natural product synthesis³⁸⁻⁴¹, the intermolecular variants—that are obviously more challenging are rarely investigated in modern synthetic chemistry. In addition, provided that the transformation could proceed, this reaction will further encounter major regio- and diastereo-selectivity issues, as inferior diastereocontrol is a general problem in the intermolecular [2+2] cycloaddition of various aromatics, such as benzothiophene²² and indole^{42,43}. Overall, from the perspective of both synthetic

¹Organisch-Chemisches Institut, Westfälische Wilhelms-Universität Münster, Münster, Germany. ²Department of Chemistry and Biochemistry, University of California, Los Angeles, CA, USA. ³Department of Chemistry, Oberlin College, Oberlin, OH, USA. ⁴These authors contributed equally: Jiajia Ma, Shuming Chen, Peter Bellotti. [™]e-mail: houk@chem.ucla.edu; glorius@uni-muenster.de

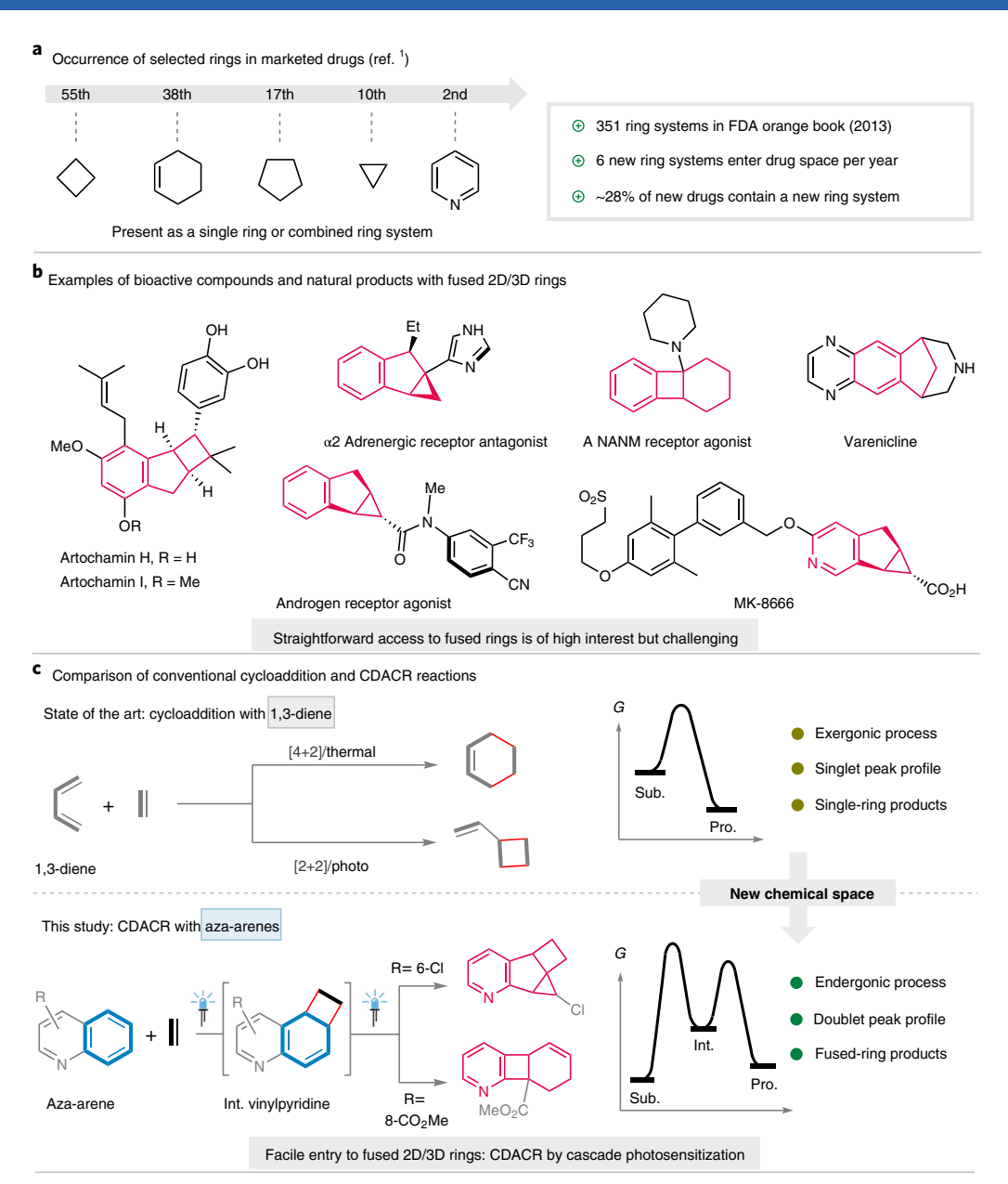


Fig. 1 Overview of 2D/3D scaffolds. **a**, Occurrence of selected rings in drugs. **b**, Examples of bioactive compounds and natural products with fused 2D/3D rings. **c**, Comparison between conventional cycloadditions and cascade dearomative cycloaddition/rearrangement (CDACR) reactions. Int., intermediate; Pro., product; Sub., substrate; FDA, US food and drug administration.

method development and its potential contribution to drug discovery, employing aromatics in cycloadditions and harnessing a consecutive transformation could lead to intriguing domains of chemical space, in compliance with the idea of diversity-oriented synthesis and skeletal diversity⁴⁴⁻⁵⁰. In this Article, we report the realization of this concept by two types of highly efficient and selective intermolecular cascade dearomative cycloaddition/rearrangement reaction of quinoline derivatives with alkenes. These reactions commence with an energy transfer (EnT)-enabled [2+2] cycloaddition of quinolines, with chloro or ester substitutions at the benzenoid rings, and are followed by either a second EnT-enabled cyclopropanation or an EnT-enabled cyclobutane rearrangement. The two consecutive EnT processes provide a straightforward approach for accessing synthetically challenging pyridine-fused polycyclic rings. The pharmaceutically relevant 3D 6-, 5-, 4- or 3-membered rings could be directly elaborated through one-shot but cascade transformations.

Results

Reaction development. In line with the previous report on dearomative [4+2] cycloaddition of quinolines with alkenes²⁹, this work started with 6-chloroquinoline (1a) and 2-chloropropene (2a), in the presence of the photosensitizer [Ir(dF(CF₃)ppy)₂(dtbbpy)][PF₆] (Ir-F, 2 mol%) (dF(CF₃)ppy, 3,5-difluoro-2-[5-(trifluoromethyl)-2-pyridinyl-N]phenyl-C; dtbby, 4,4'-di-tert-butyl-2,2'-bipyridyl) and HCl (2 equiv.), using 1,1,1,3,3,3-hexafluoropropan-2-ol (HFIP) as solvent⁵¹, under the irradiation of blue light-emitting diodes (LEDs). As a result, a structurally unique pyridine-fused 6–5–4–3 ring system (3a), which features five stereocentres—of which two are contiguous quaternary—was produced in good yield (78% yield) and with high diastereoselectivity (92:8 diastereomeric ratio (d.r.)), whereas the [4+2] cycloaddition product was not observed (Fig. 2a). Notably, the substrates 1a and 2a and the photosensitizer Ir-F are all commercially available; conversely, the produced highly

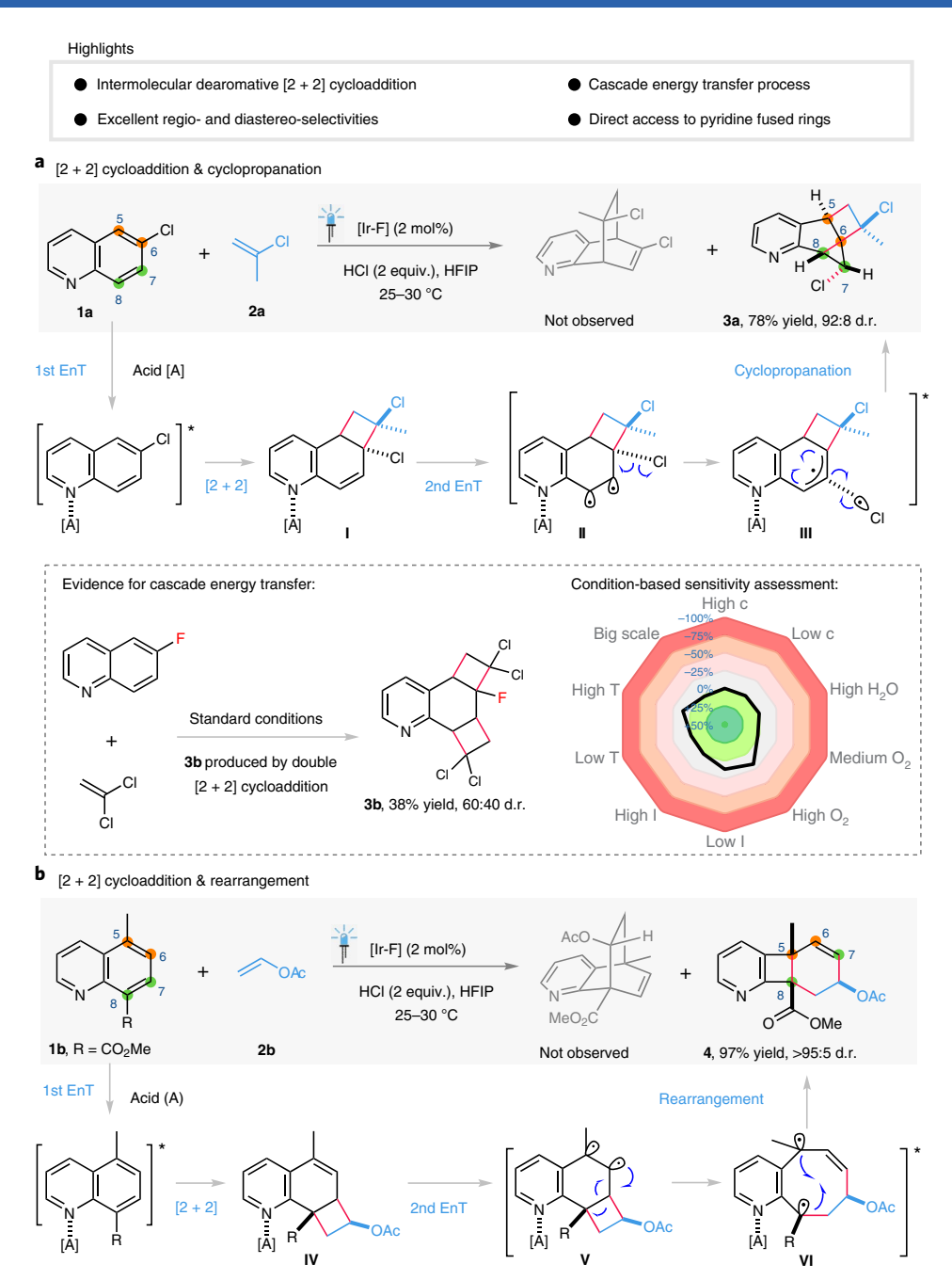


Fig. 2 | Dearomative cycloadditions of quinoline derivatives with alkenes. a, Cascade dearomative [2+2] cycloaddition/cyclopropanation reaction and the rapid assessment for its key reaction parameters. **b**, Cascade dearomative [2+2] cycloaddition/rearrangement reaction. $[Ir-F] = Ir[dF(CF_3) ppy]_2[dtbbpy](PF_6)$ (CAS No. 870987-63-6). HFIP=1,1,1,3,3,3-hexafluoropropan-2-ol. One representative enantiomer of the racemic product is presented for all throughout the text. Ac, acetyl; [A], acid additive; c, concentration; d.r., diastereomeric ratio; EnT, energy transfer; I, light intensity; T, temperature.

strained fused ring **3a** is hardly accessible through conventional synthetic methods. To enhance the reproducibility of this reaction and improve the user-friendliness, key reaction parameters were examined to assess their influence on the yields⁵². Accordingly, the concentration of substrates, moisture and scale-up did not show any notable influence on the outcome. By contrast, the reaction was negatively affected with high oxygen levels, high temperature or low light intensity. Next, methyl quinoline-8-carboxylate (**1b**) and vinyl acetate (**2b**) were subjected to the same reaction conditions thus furnishing a new type of polycyclic product, a fused 6–4–6 ring system (**4**) with excellent yield (97%) and as a single diastereoisomer (Fig. 2b). Two contiguous all-carbon quaternary centres as

the bridgeheads of the 3D 4- and 6-membered rings are efficiently generated in this reaction. Control experiments revealed that both the visible light and the photosensitizer were mandatory for these two transformations.

Mechanistic investigation. With respect to the reaction in Fig. 2a, this transformation was likely to be initiated by an energy-transfer-mediated dearomative [2+2] cycloaddition between 1a and 2a (ref. ⁵³). This gave the cinnamyl chloride analogue intermediate I (Fig. 2a), which was also detected by NMR spectroscopy. A subsequent homolytic bond dissociation of C–Cl by a second energy-transfer event furnished a triplet radical pair

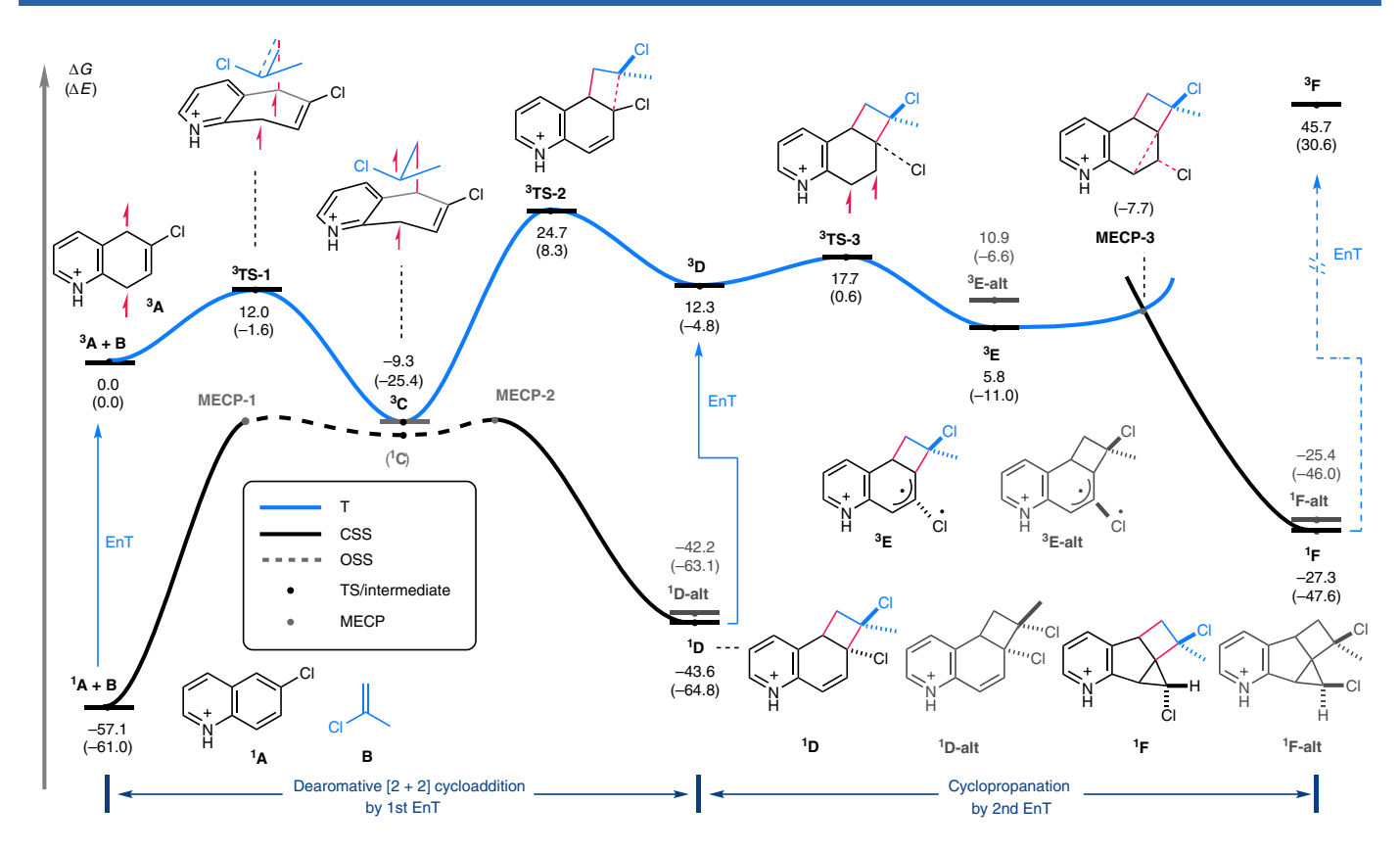


Fig. 3 | Calculated energy diagram. Values are in kcal mol $^{-1}$, obtained at the ωB97X-D/def2-TZVPP, SMD(HFIP)//ωB97X-D/def2-SVP, SMD(HFIP) level of theory for the [2+2] cycloaddition/cyclopropanation reaction sequence between 6-chloroquinoline and 2-chloropropene. T, triplet; CSS, closed-shell singlet; OSS, open-shell singlet; MECP, minimum-energy crossing point; alt, alternative diastereomer.

(from II to III). The following C-C and C-Cl bond formations furnished the terminal product 3a. Using 6-fluoroquinoline instead of the 6-chloro congener 1a, a double [2+2] cycloaddition product 3b was isolated, which provided strong evidence for the cascade energy-transfer process (Fig. 2a). Notably, all the ring formation processes proceeded in a highly diastereoselective fashion.

We investigated the mechanism of the [2+2] cycloaddition/ cyclopropanation sequence by performing density functional theory calculations on the reaction between 6-chloroquinoline (1a) and 2-chloropropene (2a) (Fig. 3). Energy transfer from the excited photosensitizer to protonated quinoline ¹A yields the triplet ³A, which readily reacts with 2-chloropropene (2a, labelled as B in Fig. 3 for clarity) via ³TS-1 on the triplet surface to form the first C-C bond with an activation free energy of 12.0 kcal mol⁻¹. As the open-shell singlet (OSS) surface lies slightly (1-2 kcal mol⁻¹) below the triplet (T) surface in energy in the vicinity of the resulting biradical intermediate ³C, ³C is most likely to undergo intersystem crossing (ISC) to the OSS biradical ¹C. The OSS surface crosses with the closed-shell singlet (CSS) surface at two minimum-energy crossing points (MECPs): MECP-1, which leads back to separated reactants and MECP-2, which furnishes the formal [2+2] cycloadduct. The chemo- and diastereo-selectivity of the reaction are therefore controlled by the rate of ISC and the OSS→CSS MECPs.

The second C–C bond formation through **MECP-2** yields [2+2] cycloadduct ¹**D**, which is 1.4 kcal mol⁻¹ more stable than its diastereomer ¹**D-alt**. Energy transfer to adduct ¹**D** under the reaction conditions gives rise to the triplet ³**D**, which can either fragment via ³**TS-2** to revert back to ³**C** or undergo homolytic C–Cl cleavage via ³**TS-3** (ref. ⁵⁴). The latter process is favoured with a low activation free energy of 5.4 kcal mol⁻¹, compared to 12.4 kcal mol⁻¹ for the C–C fragmentation. The resulting triplet radical pair ³E is more stable than its diastereomer ³E-alt as the chlorine atom prefers to

stay at the less sterically congested convex face of the fused 6-4 ring system (Supplementary Fig. 13 and Supplementary Table 5). Finally, ³E collapses to the CSS product ¹F through MECP-3, forming both the cyclopropane ring and the C–Cl bond. Due to the loss of aromaticity and the strained cyclopropane structure, ¹F is 29.8 kcal mol⁻¹ higher in free energy than the starting materials ¹A and B. Despite this, the formation of ¹F is irreversible as the triplet state from ¹F is too high in energy to be formed with the triplet sensitizer used for these reactions.

The reaction in Fig. 2b of methyl quinoline-8-carboxylate (1b) with vinyl acetate (2b) was proposed to proceed through a conceptually similar energy-transfer-mediated dearomative [2+2] pathway, leading to a vinylcyclobutane (IV). A cascade energy-transfer process triggers the ring rearrangement to produce a kinetically stable fused ring 4.

Scope and limitation. Next, we evaluated the generality of these two cascade dearomative [2+2] cycloaddition/rearrangement reactions. With respect to the [2+2] cycloaddition/cyclopropanation, commercially available 2-chloropropene derivatives were first examined and provided the corresponding fused 6-5-4-3 rings (3, 5 and 6) in good yields and diastereoselectivities (Fig. 4). An array of single-step prepared 2-chloroalkenes are compatible, demonstrating an excellent functionality tolerance, such as esters (7–11), an ether (12), fluorinated alkyl and aryl moieties (11–13), a sulfonamide derivative of the drug probenecid (14), a biphenyl (15), a benzenesulfonyl compound (16), a malonate (17), a pyridine (18) and an amide (19). 1,1-Dichloroethylene and trichloroethylene also worked smoothly thus providing polychlorinated products 20 and 21 with good results, whereas no conversion was observed using tetrachloroethylene (Supplementary Fig. 14). Comparable reaction outcomes were observed by using bromo-substituted alkenes

Fig. 4 | Substrate scope of [2+2] cycloaddition/cyclopropanation with respect to the halogenated alkenes. Reaction conditions: quinolines (0.2 mmol), alkenes (0.4 mmol or 1.0 mmol), HCl (0.4 mmol, 4 M in 1,4-dioxane) and Ir-F (2 mol%) in HFIP (1 ml) were stirred for 16 h under argon and irradiated with 30 W blue LEDs (λ_{max} = 450 nm). For experimental details, see Supplementary Methods. d.r., diastereomeric ratio; pTol, para-tolyl.

(22-25). As shown in Fig. 5, the quinoline scope of this [2+2]cycloaddition/cyclopropanation reaction was further evaluated. As a result, 6-chloroquinolines with additional substituents at any of the 2-, 3- or 4-positions exhibited excellent compatibility (26-36). The topology of the fused ring products was expanded by using tricyclic quinoline-derivative substrates (37–39). Notably, introducing one more substituent at the 5-, 7- or 8-position of 6-chloroquinoline did not hamper the reaction efficiency, thus furnishing the fused 2D/3D rings with three (40 and 41) or four (42) quaternary centres. For instance, 42 with one all-carbon quaternary centre and three fluorinated/chlorinated ones was obtained in good yield and high diastereoselectivity. 7-Chloroquinoline proved amenable to this [2+2] cycloaddition/cyclopropanation reaction (product 43) while 5- or 8-chloroquinoline did not lead to detectable amounts of products (Supplementary Fig. 14). Pleasingly, compounds 6 and 41 afforded suitable crystalline specimens and the corresponding X-ray structures are displayed to illustrate the configuration of the fused rings. The scope of the cascade dearomative [2+2]cycloaddition/rearrangement is presented in Fig. 6. The two adjacent quaternary centres (44 and 45) were formed in a highly efficient and syn-diastereoselective fashion, even in the presence of trifluoromethyl (44) or chloro (45) groups. Substitution at the pyridyl fragment was also compatible (46–50), targeting the desired product in moderate to good yields (58–82%). Good functional group tolerance was also observed in this transformation (51–59): alkenes (52, 57 and 59), an alkyne (53), a chlorinated arene (54) and a polyfluorinated alkyl (55) proved compatible with the protocol.

Synthetic application. Gram-scale reactions and derivatization of the obtained fused 6–5–4–3 and 6–4–6 rings were conducted (Fig. 7). Starting from the commercial feedstock 6-chloroquinoline and 2-bromopropene, 1.23 g of **22** was produced in 72% yield, which was comparable with the outcome of the corresponding small-scale reaction. In the presence of Pd(PPh₃)₄, under the irradiation of blue LEDs, **22** was converted to a rearomatization product (**60**). A nucleophile, lithium morpholin-4-ide could also trigger a rearomatization process by providing **61**. These two-step sequences from a halogenated quinoline and an alkene to **60** and **61** can be recognized as formal cross-electrophilic couplings. The strategy was applied towards the synthesis of an advanced intermediate (**62**) of CXCR7 receptor chemokine antagonists, offering a straightforward route towards highly decorated quinolines^{55,56}. Compound **24** can also

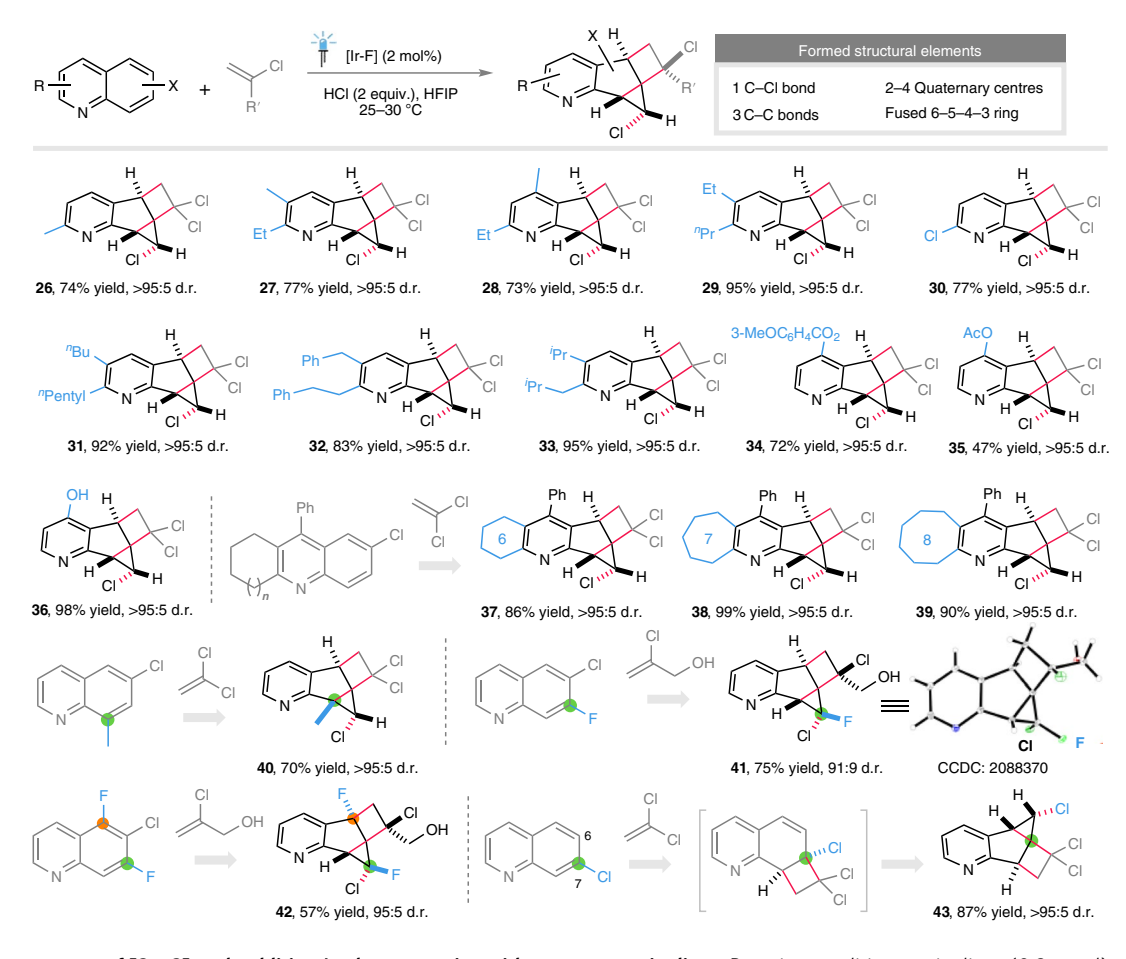


Fig. 5 | Substrate scope of [2+2] cycloaddition/cyclopropanation with respect to quinolines. Reaction conditions: quinolines (0.2 mmol), alkenes (0.4 mmol or 1.0 mmol), HCl (0.4 mmol, 4 M in 1,4-dioxane) and Ir-F (2 mol%) in HFIP (1 ml) were stirred for 16 h under argon and irradiated with 30 W blue LEDs (λ_{max} = 450 nm). For experimental details, see Supplementary Methods. Ac, acetyl; d.r., diastereomeric ratio. Orange and green circles denote specific substituted carbon atoms to help visualizing the skeletal modification events.

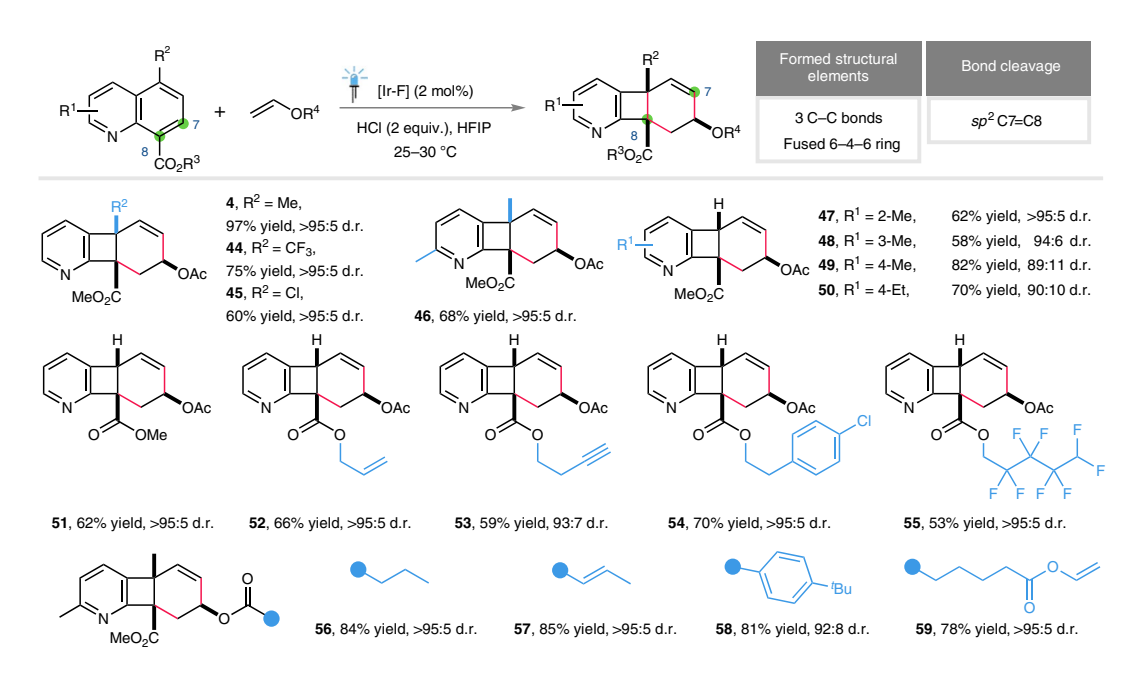


Fig. 6 | Substrate scope of [2+2] cycloaddition/rearrangement. Reaction conditions: quinolines (0.2 mmol), alkenes (1.0 mmol), HCl (0.4 mmol), 4 M in 1,4-dioxane) and Ir-F (2 mol%) in HFIP (1 ml) were stirred for 48 h under argon and irradiated with 30 W blue LEDs (λ_{max} = 450 nm). For experimental details, see Supplementary Methods. Ac, acetyl; d.r., diastereomeric ratio. Green circles highlight the formal C=C bond cleavage between C7 and C8. Light blue circles represent the substitution at the vinyl ester coupling partners.

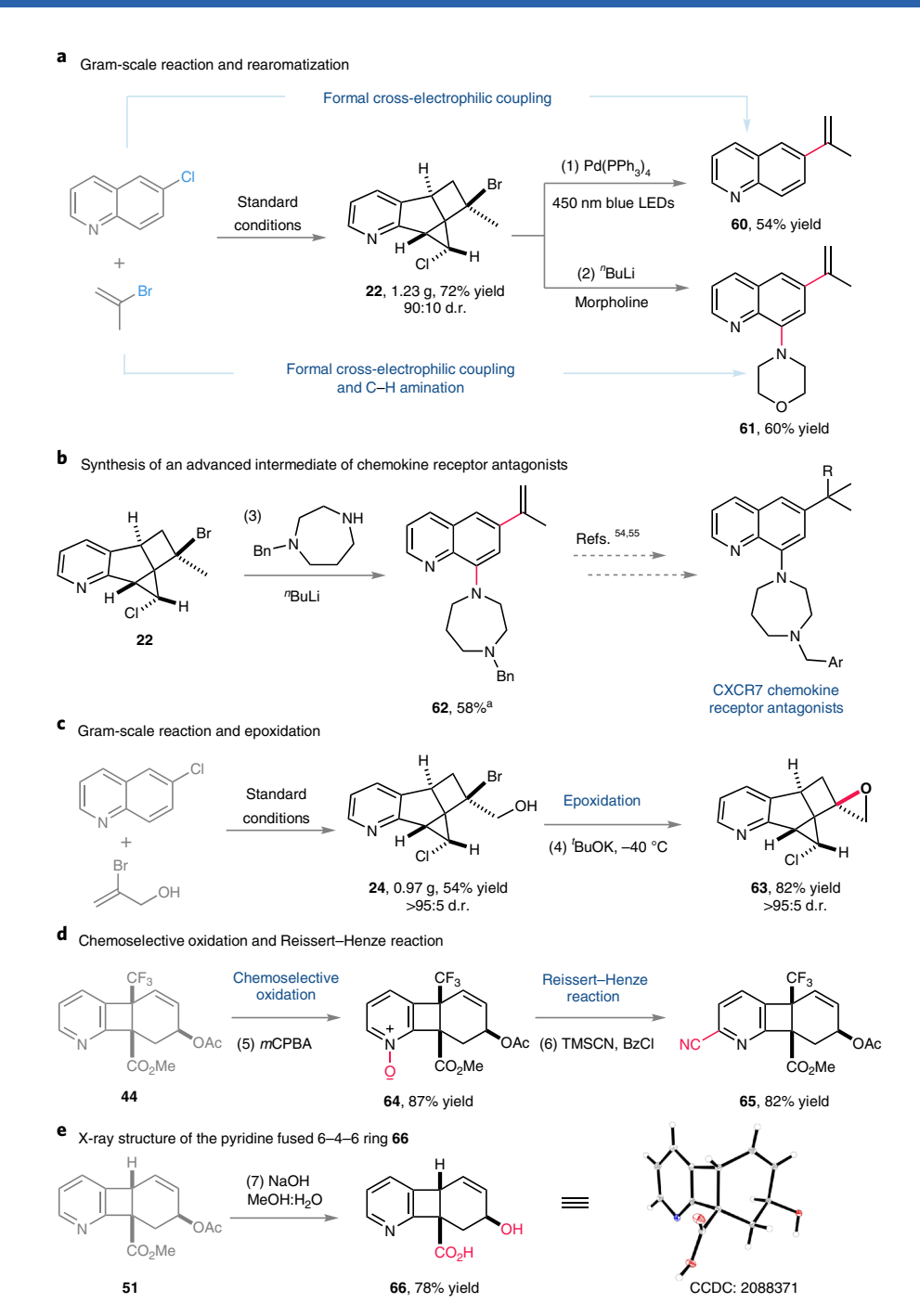


Fig. 7 | Gram-scale reactions and synthetic transformations. a, Generation of highly decorated quinolines via rearomatization. **b**, Exploitation of the rearomatization strategy forming a key intermediate towards a CXCR7 receptor antagonist. **c**, Gram-scale [2+2] cycloaddition/rearrangement reaction followed by epoxidation. **d**, Synthetic elaboration of the pyridine core via oxidation and Reissert–Henze reaction. **e**, Ester group hydrolysis and X-ray structural determination of **66**. ^a Contains approximately 15% of an inseparable isomeric product. Reaction conditions: (1) Pd(PPh₃)₄ (5 mol%), PPh₃ (10 mol%), 'BuOK (2.0 equiv.), 'PrOH (0.1 M), 450 nm LEDs, room temperature; (2) morpholine (2.0 equiv.), "BuLi (2.0 equiv.), tetrahydrofuran (THF) (0.4 M), 0 °C then **22** (1.0 equiv.), THF (0.2 M), 0 °C; (3) 1-benzyl-1,4-diazepane (2.0 equiv.), "BuLi (2.0 equiv.), THF (0.4 M), 0 °C then **22** (1.0 equiv.), THF (0.17 M), -40 °C; (5) mCPBA (3.0 equiv.), CH₂Cl₂ (0.1 M), room temperature; (6) TMSCI (3.0 equiv.), BzCI (2.0 equiv.), CH₂Cl₂ (0.1 M), 0 °C to room temperature; (7) NaOH (5.0 equiv.), MeOH:H₂O (4:1, 0.1 M), 50 °C. For experimental details, see Supplementary Methods. Bn, benzyl; Bz, benzoyl; d.r., diastereomeric ratio; mCPBA, meta-chloroperbenzoic acid; TMS, trimethylsilyl.

be synthesized in gram scale and, after treatment with 'BuOK, was converted into **63** featuring a spirocyclic epoxypropane moiety. The *meta*-chloroperbenzoic acid-mediated chemoselective oxidation of **44** gave the pyridine *N*-oxide **64** without competitive epoxidation of the cyclohexene moiety. A cyano moiety was introduced **(65)** by a subsequent Reissert–Henze reaction. Hydrolysis of **51** provided

solid **66** whose structure was resolved by X-ray analysis, thus confirming the 6-4-6 tricyclic structure.

Conclusions

We herein introduced two types of energy-transfer-mediated cascade dearomative [2+2] cycloaddition/rearrangement (CDACR)

reaction which could provide facile access to pyridine-fused 2D/3D ring systems. Tailor-made substitution at the quinoline framework could divert the second energy-transfer event towards either cyclopropanation or cyclobutane rearrangement, delivering 5–4–3-membered fused or 4–6-membered fused rings, respectively. Extremely high structural complexity was directly elaborated from readily available quinolines and alkenes by means of two consecutive energy-transfer events, mediated by an iridium-based photosensitizer. High reaction efficiency and excellent diastereoselectivity, which are challenging within the intermolecular dearomative [2+2]cycloaddition arsenal, have been observed. Furthermore, compared to the conventional cycloaddition reactions, this method using aromatics as reactants and harnessing a consecutive transformation leads to an intriguing chemical space. Given the high prevalence of pyridine-fused 2D/3D rings in drug discovery, we anticipate this method will facilitate the efficient synthesis of such scaffolds.

Methods

Representative procedure for the [2+2] cycloaddition/cyclopropanation cascade. An oven-dried 5 ml Schlenk tube was charged with the appropriate 6-chloroquinoline (1.0 equiv.), the appropriate haloalkene (2.0 or 5.0 equiv.), HCl (2.0 equiv., 4 M in 1,4-dioxane) and [Ir(dF(CF₃)ppy)₂(dtbbpy)][PF₆] (2 mol%) and 1,1,1,3,3,3-hexafluoro-2-propanol (HFIP, 0.2 M). The reaction mixture was degassed using two freeze–pump–thaw cycles. After the mixture was thoroughly degassed and filled with argon, the Schlenk tube was tightly sealed and stirred while under irradiation with 30 W blue LEDs (λ_{\max} = 450 nm) for 14–24 h (monitored by thin-layer chromatography). The reaction was quenched with saturated aqueous NaHCO₃ and extracted with CH₂Cl₂ (3 times, 10 ml each time). The organic phases were combined and concentrated under reduced pressure. ¹H NMR analysis of the crude reaction mixture gave the d.r. values. The analytically pure product was obtained by flash chromatography on silica gel (n-pentane/Et₂O or CH₂Cl₂/MeOH as eluent).

Representative procedure for the [2+2] cycloaddition/rearrangement cascade. An oven-dried 5 ml Schlenk tube was charged with the appropriate 8-quinoline ester (1.0 equiv.), the appropriate vinyl ester (5.0 equiv.), HCl (2.0 equiv., 4 M in 1,4-dioxane) and [Ir(dF(CF_3)ppy)_2(dtbbpy)][PF_6] (2 mol%) and 1,1,1,3,3,3-hexafluoro-2-propanol (HFIP, 0.2 M). The reaction mixture was degassed using two freeze–pump—thaw cycles. After the mixture was thoroughly degassed and filled with argon, the Schlenk tube was tightly sealed and stirred while under irradiation with 30 W blue LEDs (λ_{max} = 450 nm) for 48 h. The reaction was quenched with saturated aqueous NaHCO₃ and extracted with CH₂Cl₂ (3 times, 10 ml each time). The organic phases were combined and concentrated under reduced pressure. ¹H NMR analysis of the crude reaction mixture gave the d.r. values. The analytically pure product was obtained by flash chromatography on silica gel (n-pentane/EtOAc or n-pentane/acetone as eluent).

Data availability

Materials and methods, experimental procedures, mechanistic studies, computational studies, sensitivity assessment and NMR spectra are available in the Supplementary Information or from the corresponding authors upon reasonable request. CIF crystallographic data files and *xyz* coordinates of the optimized structures are available as Supplementary Information and Supplementary Data 1–7. Crystallographic data for the structures reported in this Article have been deposited at the Cambridge Crystallographic Data Centre, under deposition numbers CCDC 2088365 (6), 2088367 (26), 2088368 (29), 2088369 (30), 2088370 (41) and 2088371 (66). Copies of the data can be obtained free of charge via https://www.ccdc.cam. ac.uk/structures/.

Received: 14 July 2021; Accepted: 7 April 2022; Published online: 25 May 2022

References

- Taylor, R. D., MacCoss, M. & Lawson, A. D. G. Rings in drugs. J. Med. Chem. 57, 5845–5859 (2014).
- Aldeghi, M., Malhotra, S., Selwood, D. L. & Chan, A. W. E. Two- and three-dimensional rings in drugs. Chem. Biol. Drug Des. 83, 450–461 (2014).
- Ritchie, T. J. & Macdonald, S. J. F. The impact of aromatic ring count on compound developability – are too many aromatic rings a liability in drug design? *Drug Discov. Today* 14, 1011–1020 (2009).
- Polêto, M. D. et al. Aromatic rings commonly used in medicinal chemistry: force fields comparison and interactions with water toward the design of new chemical entities. Front. Pharmacol. 9, 395 (2018).
- Bauer, M. R. et al. Put a ring on it: application of small aliphatic rings in medicinal chemistry. RSC Med. Chem. 12, 448–471 (2021).

- Lovering, F., Bikker, J. & Humblet, C. Escape from flatland: Increasing saturation as an approach to improving clinical success. *J. Med. Chem.* 52, 6752–6756 (2009).
- Burke, M. D. & Schreiber, S. L. A planning strategy for diversity-oriented synthesis. Angew. Chem. Int. Ed. 43, 46–58 (2004).
- Krug, A. W. et al. Leveraging a clinical phase Ib proof-of-concept study for the GPR40 agonist MK-8666 in patients with type 2 diabetes for model-informed phase II dose selection. Clin. Transl. Sci. 10, 404–411 (2017).
- Hagmann, W. K. et al. Preparation of tricyclic compounds as GPR40 agonists for use in treating diabetes and associated conditions. WO patent 2014022528 (2014).
- Zhou, C., Wang, S. & Zhang, G. Fused tricyclic compounds as Raf kinase inhibitors. WO patent 2013097224 (2013).
- 11. Vacher, B. et al. Rigid analogues of the α 2-adrenergic blocker atipamezole: small changes, big consequences. *J. Med. Chem.* **53**, 6986–6995 (2010).
- Ji, Y.-Y. et al. Tying up tranylcypromine: Novel selective histone lysine specific demethylase 1 (LSD1) inhibitors. Eur. J. Med. Chem. 141, 101–112 (2017).
- Karageorgis, G., Dow, M., Aimon, A., Warriner, S. & Nelson, A. Activity-directed synthesis with intermolecular reactions: development of a fragment into a range of androgen receptor agonists. *Angew. Chem. Int. Ed.* 54, 13538–13544 (2015).
- Mollica, L. et al. Molecular dynamics simulations and kinetic measurements to estimate and predict protein-ligand residence times. J. Med. Chem. 59, 7167–7176 (2016).
- Blakemore, D. C. et al. Organic synthesis provides opportunities to transform drug discovery. Nat. Chem. 10, 383–394 (2018).
- Campos, K. R. et al. The importance of synthetic chemistry in the pharmaceutical industry. Science 363, eaat0805 (2019).
- 17. Kobayashi S. & Jørgensen, K. A. (eds) Cycloaddition Reactions in Organic Synthesis (John Wiley & Sons, 2002).
- 18. Carruthers, W. Cycloaddition Reactions in Organic Synthesis (Elsevier, 2013).
- 19. Hu, N. et al. Catalytic asymmetric dearomatization by visible-light-activated [2+2] photocycloaddition. *Angew. Chem. Int. Ed.* **57**, 6242–6246 (2018).
- James, M. J., Schwarz, J. L., Strieth-Kalthoff, F., Wibbeling, B. & Glorius, F. Dearomative cascade photocatalysis: divergent synthesis through catalyst selective energy transfer. J. Am. Chem. Soc. 140, 8624–8628 (2018).
- Zhu, M., Zheng, C., Zhang, X. & You, S.-L. Synthesis of cyclobutane-fused angular tetracyclic spiroindolines via visible-light-promoted intramolecular dearomatization of indole derivatives. J. Am. Chem. Soc. 141, 2636–2644 (2019).
- Strieth-Kalthoff, F. et al. Discovery of unforeseen energy-transferbased transformations using a combined screening approach. *Chem* 5, 2183–2194 (2019).
- Ma, J. et al. Direct dearomatization of pyridines via an energy-transfercatalyzed intramolecular [4+2] cycloaddition. Chem 5, 2854–2864 (2019).
- Oderinde, M. S. et al. Synthesis of cyclobutane-fused tetracyclic scaffolds via visible-light photocatalysis for building molecular complexity. J. Am. Chem. Soc. 142, 3094–3103 (2020).
- Zhu, M., Xu, H., Zhang, X., Zheng, C. & You, S.-L. Visible-light-induced intramolecular double dearomative cycloaddition of arenes. *Angew. Chem. Int.* Ed. 133, 7112–7116 (2021).
- Zhuang, W., Cheng, Y.-Z., Huang, X.-L., Huang, Q. & Zhang, X. Visible-light induced divergent dearomatization of indole derivatives: controlled access to cyclobutane-fused polycycles and 2-substituted indolines. *Org. Chem. Front.* 8, 319–325 (2021).
- Mu, X.-P. et al. Stereoselective synthesis of cyclohepta[b]indoles by visible-light-induced [2+2]-cycloaddition/retro-Mannich-type reactions. Angew. Chem. Int. Ed. 60, 11211–11216 (2021).
- Oderinde, M. S. et al. Photocatalytic dearomative intermolecular [2+2] cycloaddition of heterocycles for building molecular complexity. *J. Org. Chem.* 86, 1730–1747 (2021).
- Ma, J. et al. Photochemical intermolecular dearomative cycloaddition of bicyclic azaarenes with alkenes. Science 371, 1338–1345 (2021).
- Huck, C. J. & Sarlah, D. Shaping molecular landscapes: recent advances, opportunities, and challenges in dearomatization. Chem 6, 1589–1603 (2020).
- Oderinde, M. S. et al. Advances in the synthesis of three-dimensional molecular architectures by dearomatizing photocycloadditions. *Tetrahedron* 103, 132087 (2022).
- Zheng, C. & You, S.-L. Advances in catalytic asymmetric dearomatization. ACS Cent. Sci. 7, 432–444 (2021).
- Strieth-Kalthoff, F., James, M. J., Teders, M., Pitzer, L. & Glorius, F. Energy transfer catalysis mediated by visible light: principles, applications, directions. *Chem. Soc. Rev.* 47, 7190–7202 (2018).
- Metternich, J. B. & Gilmour, R. One photocatalyst, n activation modes strategy for cascade catalysis: emulating coumarin biosynthesis with (-)-riboflavin. J. Am. Chem. Soc. 138, 1040-1045 (2016).
- Wagner, P. J. Photoinduced ortho [2+2] cycloaddition of double bonds to triplet benzenes. Acc. Chem. Res. 34, 1–8 (2001).
- Hoffmann, N. Photochemical cycloaddition between benzene derivatives and alkenes. Synthesis 481–495 (2004).

- Remy, R. & Bochet, C. G. Arene-alkene cycloaddition. Chem. Rev. 116, 9816–9849 (2016).
- Zech, A., Jandl, C. & Bach, T. Concise access to the skeleton of protoilludane sesquiterpenes through a photochemical reaction cascade: total synthesis of atlanticone C. Angew. Chem. Int. Ed. 58, 14629–14632 (2019).
- Schneider, F., Samarin, K., Zanella, S. & Gaich, T. Total synthesis of the complex taxane diterpene canataxpropellane. Science 367, 676–681 (2020).
- Roche, S. P. & Porco, J. A. Jr Dearomatization strategies in the synthesis of complex natural products. *Angew. Chem. Int. Ed.* 50, 4068–4093 (2011).
- Zhang, Z., Zhou, Y.-J. & Liang, X.-W. Total synthesis of natural products using photocycloaddition reactions of arenes. *Org. Biomol. Chem.* 18, 5558–5566 (2020).
- Ikeda, M., Ohno, K., Mohri, S.-i., Takahashi, M. & Tamura, Y. Regio- and stereo-chemical aspects of [2 + 2] photocycloaddition between 1-benzoylindoles and olefins. *J. Chem. Soc. Perkin* 1, 405–412 (1984).
- Ma, J. et al. Gadolinium photocatalysis: dearomative [2+2] cycloaddition/ringexpansion sequence with indoles. Angew. Chem. Int. Ed. 59, 9639–9645 (2020).
- Wender, P. A. & Howbert, J. J. Synthetic studies on arene-olefin cycloadditions: total synthesis of (+)-alpha-cedrene. J. Am. Chem. Soc. 103, 688–690 (1981).
- 45. Kuznetsov, D. M., Mukhina, O. A. & Kutateladze, A. G. Photoassisted synthesis of complex molecular architectures: dearomatization of benzenoid arenes with aza-o-xylylenes via an unprecedented [2+4] reaction topology. *Angew. Chem. Int. Ed.* 55, 6988–6991 (2016).
- Southgate, E. H., Pospech, J., Fu, J., Holycross, D. R. & Sarlah, D. Dearomative dihydroxylation with arenophiles. *Nat. Chem.* 8, 922–928 (2016).
- Næsborg, L., Jandl, C., Zech, A. & Bach, T. Complex carbocyclic skeletons from aryl ketones through a three-photon cascade reaction. *Angew. Chem. Int. Ed.* 59, 5656–5659 (2020).
- Park, S. & Chang, S. Catalytic dearomatization of N-heteroarenes with silicon and boron compounds. Angew. Chem. Int. Ed. 56, 7720–7738 (2017).
- Cornelisse, J. The meta photocycloaddition of arenes to alkenes. *Chem. Rev.* 93, 615–669 (1993).
- 50. Jiang, Y. et al. Advances in polycyclization cascades in natural product synthesis. *Chem. Soc. Rev.* **50**, 58–71 (2021).
- Pozhydaiev, V., Power, M., Gandon, V., Moran, J. & Lebœuf, D. Exploiting hexafluoroisopropanol (HFIP) in Lewis and Brønsted acid-catalyzed reactions. *Chem. Commun.* 56, 11548–11564 (2020).
- Pitzer, L., Schäfers, F. & Glorius, F. Rapid assessment of the reactioncondition-based sensitivity of chemical transformations. *Angew. Chem. Int.* Ed. 58, 8572–8576 (2019).
- 53. Döpp, D. & Jung, A. Photocycloaddition of 2-morpholinopropenenitrile to 8-acetylquinoline. *Acta Chim. Slov.* **56**, 664–668 (2009).
- Xu, B. et al. Photocatalyzed diastereoselective isomerization of cinnamyl chlorides to cyclopropanes. J. Am. Chem. Soc. 142, 6206–6215 (2020).
- 55. Chen, X. et al. Modulators of CXCR7. WO patent 2010054006 (2010).
- Gotoh, N. & Campbell, J. J. CCR7 chemokine receptor antagonists for the treatment of cancer. WO patent 2020123582 (2020).

Acknowledgements

We thank J.-H. Ye and F. Strieth-Kalthoff (all WWU) for assistance and discussions. Generous financial support from the Deutsche Forschungsgemeinschaft (SFB 858, Leibniz Award) and the European Research Council (ERC Advanced Grant Agreement no. 788558) is gratefully acknowledged. K.N.H. thanks the National Science Foundation (Grant CHE-1764328) for financial support. Calculations were performed on the Hoffman2 cluster at the University of California, Los Angeles and the Extreme Science and Engineering Discovery Environment (XSEDE), which is supported by the National Science Foundation (Grant OCI-1053575).

Author contributions

F.G., J.M. and P.B. conceived the project. J.M., P.B. and T.W. performed the synthetic experiments. S.C. performed the density functional theory calculations. C.D. analysed the X-ray structures. J.M., S.C., K.N.H. and F.G. supervised the research and wrote the manuscript with contributions from all authors.

Funding

Open access funding provided by Westfälische Wilhelms-Universität Münster

Competing interests

The authors declare no competing interests.

Additional information

Supplementary information The online version contains supplementary material available at https://doi.org/10.1038/s41929-022-00784-5.

Correspondence and requests for materials should be addressed to Kendall N. Houk or Frank Glorius

Peer review information *Nature Catalysis* thanks Taye Demissie and the other, anonymous, reviewer(s) for their contribution to the peer review of this work.

Reprints and permissions information is available at www.nature.com/reprints.

Publisher's note Springer Nature remains neutral with regard to jurisdictional claims in published maps and institutional affiliations.



Open Access This article is licensed under a Creative Commons Attribution 4.0 International License, which permits use, sharing, adaptation, distribution and reproduction in any medium or format, as long

as you give appropriate credit to the original author(s) and the source, provide a link to the Creative Commons license, and indicate if changes were made. The images or other third party material in this article are included in the article's Creative Commons license, unless indicated otherwise in a credit line to the material. If material is not included in the article's Creative Commons license and your intended use is not permitted by statutory regulation or exceeds the permitted use, you will need to obtain permission directly from the copyright holder. To view a copy of this license, visit http://creativecommons.org/licenses/by/4.0/.

© The Author(s) 2022